Research on Grid Positioning Strategy of Coupling Mechanism in Wireless Charging System With Offset Angle Variable

Linlin Tan, *Member, IEEE*, Yongfeng Yu, Jiaqi Wang, Ruoyin Wang, and Chengyun Li

***Abstract*—The precise positioning of receiving and transmitting coils of the wireless power transmission system is the precondition for its efficient operation, and it is necessary and indispensable in practice. The novel grid positioning model and algorithm of four pick-up coils with angles is established by adding the deflection angle of the receiving coil. The corresponding relationship between space magnetic field and pickup coil voltage is analyzed, and the method of magnetic field reconstruction is studied in this article. Then, considering the sampling workload and effectiveness of pick-up coil voltages at grid point, the pick-up coil voltages were reconstructed and expanded based on variable slope interpartition sampling and Kriging interpolation, to increase the positioning database. It is found that the positioning accuracy of receiving coil can be improved with the grid sampling interval density increasing, or by using variable slope sampling while the number of grid sampling is unchanged. Under the grid sampling interval of 2.5 cm, the average positioning error of the system is less than 1 cm in this article, and the experimental results are basically consistent with the theoretical results, and the validity of the proposed approach is verified.**

***Index Terms*—Coil positioning, grid positioning model and algorithm, variable slope sampling, wireless charging system.**

I. Introduction

WIRELESS power transmission (WPT) technology for electric vehicles (EVs) has the characteristics of flexibility, convenience, and efficiency [1], [7], [8], [9]. In addition to the main power circuits such as power conversion device, coupling mechanism coils, and compensation network, the reliable and safe operation of EV WPT system also requires relevant auxiliary technical support, such as foreign object detection technology and alignment guidance technology.

Currently, in the relevant standards of EV WPT, the Society of Automotive Engineers (SAE) standard SAEJ2954 and the Chinese standard GB/T 38775.1 have detailed provisions on the acceptable offset of the receiving and transmitting coils [2]. For example, GB/T 38775.1 requires that the center alignment of the receiving and transmitting coils should be taken as (see Fig. 1): in the X-axis direction, the displacement is required to be within the range of ± 75 mm, which is required to be within the range of ± 100 mm in the Y-axis direction, that can be ensure that the efficiency of the electric vehicle charging system is not less than 80%. But research shows that the average coil misalignment exceeds 70 cm [3] if the driver lacks auxiliary equipment, which is much higher than the limit of coil antioffset of standards. Without any information feedback of the positioning assistance system for parking correction, it is difficult to complete such a fine position docking by artificial intuition [4], [5], [6]. Therefore, it is very important and necessary to accurately obtain the position relationship between the receiving and transmitting coils, and provide feedback for the driver or the positioning assistance system to achieve effective parking.

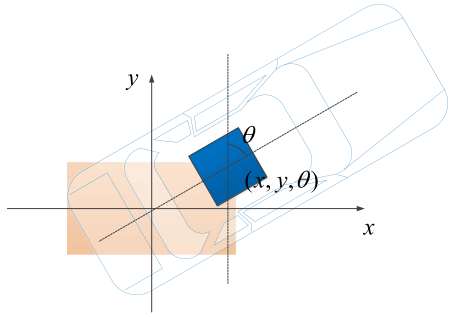

Fig. 1. Wireless charging offset of electric vehicles.

The research on positioning technology of wireless charging system mainly focuses on two types of technical directions. The first is performed by attaching optical sensors, ultrasonic sensors, RFID, magnetic sensors and other devices, and positioning through machine vision and triangulation and other algorithms. The method sometimes is vulnerable to interference from the external environment, such as rain, snow, sand, and dust, the reliability of positioning needs to be improved [7], [8], [9], [10], [11], [12], [13], [14]. The other is to use the electromagnetic characteristics of the WPT system itself to locate the position [15], [16], [17], [18], [19], [20], [21], [22], [23], [24], [25], [26], [27], [28], by studying the influence of the offset on the parameters of the receiving and transmitting coils or the change of the space magnetic field. The advantages of this method are simple, effective, practical, and low cost.

Manuscript received 13 October 2022; revised 22 December 2022; accepted 7 January 2023. Date of publication 18 January 2023; date of current version 10 March 2023. This work was supported by the National Key Research and Development Program under Grant 2021YFB2501600. Recommended for publication by Associate Editor J. Biela. *(Corresponding author: Linlin Tan.)*

The authors are with the School of Electrical Engineering, Southeast University, Nanjing 210096, China (e-mail: tanlinlin@seu.edu.cn; 220213129@seu.edu.cn; 2565490567@qq.com; ruoy_wang@yahoo.com; lc.yun@foxmail.com).

Color versions of one or more figures in this article are available at https://doi.org/10.1109/TPEL.2023.3237901.

Digital Object Identifier 10.1109/TPEL.2023.3237901

It is one of the current mainstream orientation directions. For example, through the impact of the position offset of the transmitting and receiving coils on the voltage and current phase of the transmitting inverter, a database of impact relationship is built. With four small pick-up coils, direction identification is assisted to achieve high-precision positioning, and the maximum positioning error within 5 cm [15]. The Texas A&M research group proposed a method to estimate the offset in each direction using the differential voltage of two pairs of detection coils. Combined with the closed-loop control, the alignment of the transmitting, and the receiving coils is realized. This processing method bypassed the calculation of the position coordinates on the receiving coil, and achieved the coil alignment by the negative feedback closed-loop control [16], [17].

In the research of positioning based on the electromagnetic characteristics of the system itself, high-precision positioning can also be achieved by installing a certain number of pickup coils. Literature [18], four pick-up coils with symmetric arrangement were used, and the localization space was divided into multiple grids. At each grid point, the induction values of four pickup coils without angle offset are collected simultaneously. A group of voltage matrices are constructed at each grid point. Then, the position of the receiving coil can be obtained by using the table lookup method. Combined with the position correction algorithm, the two degrees of freedom precise positioning of X and Y coordinates in the plane is realized. An accurate circuit model for the coupling of four detection coils to the power coil was constructed in the literature [19], with a positioning accuracy of 1 cm. Triple-coil-structure-based coil positioning system were also studied, and the coil positioning with error was less than 1.5 cm [20].

In addition, researchers have also conducted lots of research [21], [22], [23] on the layout scheme and shape of the pickup coils, and some researchers have also designed relay coils, new types of coils, so as to achieve higher accuracy of electromagnetic positioning [24], [25], [26], which laying a technical foundation for positioning using the electromagnetic characteristics of the wireless charging system.

Considering the practical situation of electric vehicle parking, there may be external deflection in X and Y directions during parking. The method constructed in literature [18] is no longer applicable. The positioning algorithm is easy to fail, and the positioning error will be large or uncontrollable while the transmitting and receiving coils are deflected, Because of the randomness of the deflection angles of the transmitting and receiving coils, we cannot measure all the possible values of the pickup coil' voltages at the same grid point, therefore, the construction of the pickup coil voltage database can no longer be done in groups. The voltage database of pick-up coil should be to build separately at each grid point, and the positioning algorithm also needs to be redesigned. Sometimes, in the symmetrical space magnetic field, the results of the existing positioning algorithm of four pick-up coil is not unique if angular deflection occurs, and the reason will be discussed in the following.

In summary, a high-precision positioning algorithm for four pickup coils with deflection angle is redesigned, and the solution method and positioning constraint equation with angle information is established. Compared with the existing four coil positioning strategy [18], [19], it will bring cost increase of the positioning system, although cost increased, but increase is limited after all. The gyroscope modular is selected in this article only a few dollars. It is necessary to obtain angle in practice, which will bring more friendly positioning effect and more practicality. Meanwhile, this article avoids the complex secondary correction calculation of the location coordinates of the receiving coil, and uses the interpolation method to expand the location grid. It simplifies the complexity of the algorithm and makes the implementation more efficient, the differences between the methods described in this article and the existing algorithms was shown in Table I.

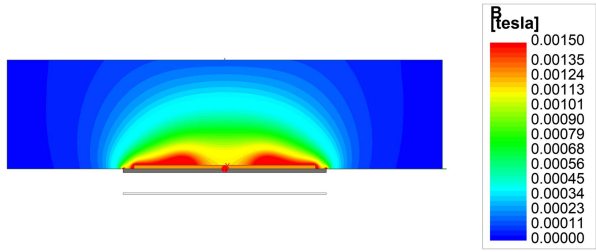

Fig. 2. Planar magnetic field distribution of the transmitting coil ($x = 0$, $-330<y<300$, $0<z<150$, unit: mm, simulation parameters: the size of the square planar spiral coil is 300 mm, the inner diameter is 160 mm, the number of turns is 10, and the excitation current is 10 A.

II. Magnetic Field Analysis of Unipolar Coil and Principle of Discretized Coil Positioning

In order to ensure charging efficiently, the receiving and transmitting coils positioning of the electric vehicle needs to be completed before charging. During the positioning process, the inverter of the wireless charging system can be adjusted to generate a stable current for the transmitting coil, so as to stimulate a stable magnetic field. Normally, the receiving coil is disconnected during the positioning process, only the pickup coils works. After the positioning is completed, the pickup coils system will no longer work.

Take a square planar spiral coil as an example, which produces a unipolar distributed magnetic field (except at the edges) under the excitation of certain stable high frequency current (see Fig. 2). The spatial magnetic field is basically symmetrical, and the magnetic field intensity at the center reaches a maximum. It is obvious that the magnetic flux density at each (x, y) coordinate and the same height under a constant current excitation is constant. This is also effectively illustrated by Fig. 2, which gives the magnetic field distribution of a rectangular coil for a certain parameter.

A. Discrete Pickup Coil Positioning Principle and Algorithm

Neglecting the effect of intercoil capacitance, for an N-turn spiral coil, the z-axis component of the magnetic flux density at any point in space under the excitation of the current I can be

TABLE I
COMPARISON OF POSITIONING MODELS

literature	Positioning principle	Pick-up number	Coil type	Angle compatibility	Positioning accuracy
[15]	Using inverter output phase change for positioning, and the pickup coil is used for direction correction	4	Circular	Yes	5cm
[16-17]	Positioning by using the difference value change of pickup coil	4	Qi charger	/	1.2cm
[18]	Four pickup coils without angle offset are collected at each grid point simultaneously; look up the table for positioning with pick-up coils, Coordinates need to be corrected	4	Circular/ Square	No	3cm
[19]	Build a grid database of pickup coils, and look up the table for positioning with four pick-up coils	4	Square	No	1cm
[20]	Triple-Coil-Structure coil positioning with 6 pick-up coils, located on the transmitting coil, Placed on the transmitting coil	6	standard J2954	No	1.5cm
This article	Constructed separately at each grid point; compatible with any angle, the grid point density is expanded by using the method of mathematical difference	4	Circular/ Square	Yes	1.2cm

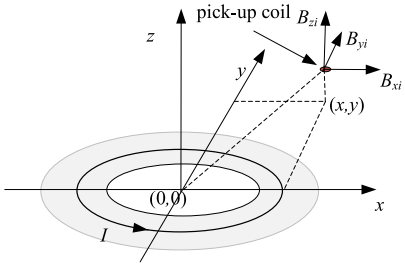

Fig. 3. Decomposition of the spatial magnetic field of the energized coil.

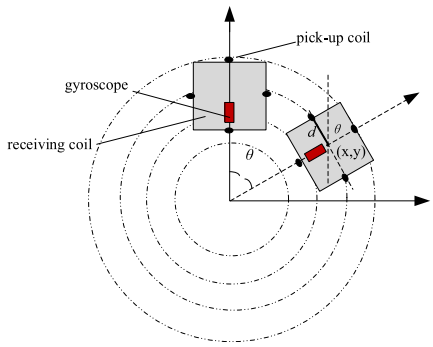

Fig. 4. Specific deflection of coil symmetrical magnetic field.

approximated as

$$\dot{B}_{zp} = \sum_{i=1}^{N} B_{zi}. \tag{1}$$

In (1), B_{zi} is the z-axis component of the magnetic induction intensity of a single-turn coil at a point. As shown in Fig. 3, when the receiving coil loop of wireless charging system is disconnected, the transmitting coil generates a relatively stable magnetic field in space.

The pickup coils installed in the receiving coil is generally parallel to the receiving coil plane, and the cross-sectional area is much smaller than the transmitting and receiving coils', which can be considered as a tiny surface element, so the pickup coil can be considered to pass only the magnetic lines of force in the z-axis direction. It is worth noting that when the receiving coil installed with the pickup coil is located at different positions above the transmitting coil, it will theoretically have a certain impact on the magnetic field of the transmitting coil. If only a fixed plane with $z = Z_0$ is considered, this impact will not affect the monopolar distribution characteristics of the magnetic field somewhere. There is the correspondence between the pickup coils above the magnetic field and its spatial position, assuming that the pickup coil induced voltage is U_{di}, then according to the law of electromagnetic induction, it can be obtained

$$\dot{U}_{di} = N_d \frac{d\phi_{di}}{dt} = N_d \frac{d}{dt} \sum_{j=1}^{N_p} \iint_{\Omega_i} \dot{B}_{zp} dx dy \left\{ \Omega_i | (x - x_{di})^2 + (y - y_{di})^2 \le r_d, z = z_{di} \right\}. \tag{2}$$

In (2), Ω is the surface element area of the position pickup coil itself that allows the passage of magnetic flux, N_d is the number of turns of the pickup coil, N_p is the number of turns of the transmitting coil, and (x_{di}, y_{di}) is the coordinate of the center point of the pickup coil. From (2), it can be seen that when the excitation current of the transmitting coil is constant, the voltage induced by the position pickup coil at each position in the xyZ_0 plane will correspond to its position coordinates (x_{di}, y_{di}). If we create a database of the pickup coil induction voltage and its possible position coordinates under a constant magnetic field generated by a certain transmitting coil, then in the actual positioning, the measured induction voltage is used to find the possible position coordinates in the database, and if the position coordinates mathematically satisfy the realistic constraint relationship, then the coordinates of each pickup coil will be found, and then the position information of the receiving coil can be obtained, which is the theoretical basis of pickup coil positioning. When using pick-up coils for positioning, a minimum of three should be arranged. While increasing the number of pickup coils can improve the accuracy, it also requires more complex solution algorithms.

The positioning scheme based on four pickup coils is shown in Fig. 4, the circular dotted line is the contour of the magnetic field intensity generated by the transmitting coil in the Z_0 plane, and the dotted lines with different radii represent different magnetic fields value. In the case of deflection, it is not difficult to find that the induced voltage on the four pickup coils is the same

before and after the angle deflection of the receiving coil occurs in space. Therefore, it is very difficult to analyze the deflection angle from using the method of looking up the corresponding relationship database of the induced voltage and position. Because the solution of the positioning equation is not unique, and the positioning algorithm of the coil will become invalid at this time. To solve this problem, this article obtains the deflection angle between the receiving and transmitting coils through the gyroscope. The installation of the gyroscope and the detection coil is shown in Fig. 4.

The gyroscope direction is consistent with the secondary coil axis. The angle is taken as a constant variable to rebuild the positioning algorithm. Assuming that the distance between the position pickup coil and the center of the receiving coil (x, y) is d, and the coordinates of the center point of the receiving coil are (x, y, Z), and the deflection angle of the receiving coil is θ_0, It is not difficult to obtain the constraint equations with (3). In (3), (x_{di}, y_{di}) is the coordinates of the center point of each pickup coil, which can be approximated as the coordinates of the pickup coil due to its small size. In (3), the coordinates (x, y) of the receiving coil are the variables to be solved, d and θ_0 are known quantities

$$\begin{cases} x_{d1} = x + d\ \sin\ \theta_0,\ y_{d1} = y + d\ \cos\ \theta_0 \\ x_{d2} = x - d\ \cos\ \theta_0,\ y_{d2} = y + d\ \sin\ \theta_0 \\ x_{d3} = x - d\ \sin\ \theta_0,\ y_{d3} = y - d\ \cos\ \theta_0 \\ x_{d4} = x + d\ \cos\ \theta_0,\ y_{d4} = y - d\ \sin\ \theta_0. \end{cases} \tag{3}$$

If we want to accurately solve (3), (2) and through magnetic field calculation, establish the relationship between the induced voltage value of the pickup coil and its spatial position. However, the solution of (2) is a nonlinear, multiple integration problem, which requires a large amount of calculation, and it is difficult to solve it directly in engineering. Therefore, the distribution of the space magnetic field of the transmitting coil in (2) on the z-axis is discretized, and the continuous z-axis magnetic field in the space area is divided into a set of grid points according to a certain step size. Furthermore, (2) is rewritten as

$$U_{\mathrm{di}} = N_d \frac{d}{dt} \sum_{j=1}^{N_p} \sum_{q=1}^{P} B_{ziq} S_q, n\ =\ 1, 2, 3, 4. \tag{4}$$

In (4), B_{ziq} is the z-axis component of the magnetic flux density at the location of the pickup coil, P is the number of discrete elements in the cell area, and S_q is the area of discrete elements. It's not hard to find the magnetic field at the grid point corresponds to the induced voltage of the pickup coil one by one, and the magnitude of the magnetic field at this point maps to the position coordinate. After gridding, we can set different number of grid sampling points to collect the voltage value of the pickup coil and form a database of the pickup coil voltage position relationship. The specific implementation principle is shown in Fig. 5. In Fig. 5, the dotted line is the grid point constructed in this article, and its coordinates have been set and unique according to the position of the transmitting coil. Suppose that the induced voltage values of the four pickup coils on the receiving coil measured are U_{d1}, U_{d2}, U_{d3}, U_{d4}, respectively, and the coil deflection angle is θ_0.The ergodic method is used

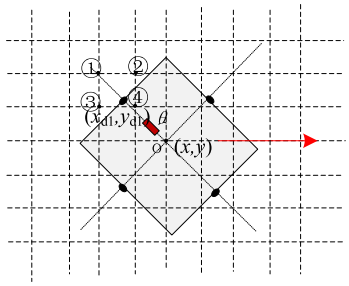

Fig. 5. Schematic diagram of positioning principle.

to solve the coordinates (x, y) of the receiving coil along a fixed step (generally less than the grid point spacing). Taking Fig. 5 as an example, when the coordinates (x, y) of the central point of the receiving coil traverse to the position shown in the Fig. 5, it is not difficult to calculate the coordinates $(x_{\mathrm{d1}}, y_{\mathrm{d1}})$ of pickup coil through the deflection angle θ_0 and (3). According to this coordinate, the pick-up coil' position is determined to be between grid points ①–④. Due to the grid is small enough in this article, the theoretical voltage U_{d1mn} of pickup coil 1 is approximated by the average voltage of grid points ①–④, that is

$$U_{d1mn}\left(x_{d1}, y_{d1}\right) \approx \frac{1}{4}\left[U\left(x_1, y_1\right) + U\left(x_2, y_2\right) + U\left(x_3, y_3\right) + U\left(x_4, y_4\right)\right]. \tag{5}$$

If the position of pickup coil happens to be on a grid point, then the theoretical value of the induced voltage of the pickup coil is the same as the sampling voltage at the grid point. If it is on the grid line, the average value is calculated according to the voltage of the two nearest points on the grid line. In the same way, the theoretical voltage values of the remaining pickup coils when the coordinates of the center point of the receiving coil are (x, y) can be obtained, respectively, and the theoretical voltage value matrix of the pickup coil at the current grid point can be constructed

$$u\left(x_m, y_n, \theta\right) = \begin{bmatrix} u_{d1mn}\left(x_{d1}, y_{d1}\right) \\ u_{d2mn}\left(x_{d2}, y_{d2}\right) \\ u_{d3mn}\left(x_{d3}, y_{d3}\right) \\ u_{d4mn}\left(x_{d4}, y_{d4}\right) \end{bmatrix}. \tag{6}$$

Use the actual measured value of the pickup coil here to calculate the position error function ε

$$\varepsilon\ = \|u - u\left(x_m, y_n\right)\| = \sum_{i=1}^{4} \left|u_{di} - u_{dimn}\right|. \tag{7}$$

When the coordinates (x, y) of the center point of the receiving coil completely traverse all grid points, and find out the position error function ε. The smallest point is the position coordinate of the receiving coil, and the gyroscope display is the angular offset of transmitter and receiver coils

However, in the abovementioned positioning method, the positioning accuracy depends very much on the density of the grid points. The denser the grid points built before positioning, the higher positioning accuracy.

B. Gridded Equivalent Magnetic Field Distribution Acquisition and Grid Point Setting

In order to obtain higher positioning accuracy, in [18], the coordinates (x, y) of the central point of the receiving coil were initially located by the calendar method and table lookup method. Then through the position relationship between the center point and grid coordinates, the center point coordinate is modified by different weight factor of the grid position. In this article, the interpolation method is used to increase the construction density of grid points to improve the positioning accuracy. In fact, the induced voltage measurement of the pickup coil at the grid point of the electric vehicle WPT system can be completed with high-precision test bench before leaving the factory, and the test step can reach millimeter level. During the test, a constant excitation current is applied to the transmitting coil. Within the moving range, the grid step is set to keep the distance between the z-axis of the receiving and transmitting coils unchanged. The induced voltage of the pickup coil at each grid point is measured in turn, and the position coordinates and the induced voltage value at that point are recorded. For more accurate data, the influencing factors of the electric vehicle chassis (such as adding auxiliary steel plates and equivalent shielding materials) can be introduced during the test to obtain more practical data.

As an example, if a 10×10 gridded point measurement is taken, 100 measurements are needed to fully obtain the data of each grid point, and when the grid density increases to 30×30, 900 precise measurements are needed, which shows that the data collection workload increases geometrically. Obviously, if the grid density is too small, it is not realistic to actually measure.

For any grid point position (x_{i}, y_{i}), the magnetic field B_{zi} is stable, and the induced voltage of the pickup coil under this stable magnetic field is also a stable value. Therefore, the induced voltage value at the grid point can be converted by a fixed coefficient to characterize the magnetic field, as shown in

$$\begin{cases} (x_i, y_i) \to B_{zi}(x_i, y_i) \rightleftarrows U(x_i, y_i) \\ U(x_i, y_i) = \alpha B_{zi}(x_i, y_i). \end{cases} \tag{8}$$

In actuality, if the pickup coil happens to locate between any two discrete points, the pickup coil induced voltage may vary due to small changes in the magnetic field. Considering that the changes in the magnetic field between any two points has continuity, the change of the magnitude of the pickup coil induced voltage should also have the same change law. The magnetic field between the actual grid measurement points can be mathematically further constructed and improved by using mathematical interpolation methods. Those mathematical interpolation methods can also be applied to reconstrue the measured voltage between grid points, which is to expand the density of grid points and improve the positioning accuracy.

III. Analysis of Magnetic Field Reconstruction Method of Wireless Charging Coil

The main purpose of this section is to recover the magnetic field distribution in space from a small amount of known discrete point data, and thus, to extend the data between actual grid points

A. Interpolation Method Selection

In this article, linear interpolation, cubic spline function interpolation, and Kriging interpolation are analyzed in order to select a suitable interpolation algorithm for magnetic field reconstruction.

Linear interpolation uses a linear function as an interpolation function, which is stable, simple to compute. Suppose two points (x_1, y_1), (x_2, y_2) are known, and the curve of other point functions between these two points is

$$y = \frac{y_2 - y_1}{x_2 - x_1} x + \frac{x_2 y_1 - x_1 y_2}{x_2 - x_1}. \tag{9}$$

The interpolation function is a straight line and this method is simple in principle and has a good interpolation effect for distribution curves with linear rate of change characteristics.

The triple spline function interpolation has excellent numerical stability and curve smoothness, which is widely used.

If $a = x_0 < x_1 < \cdots < x_n\text{-}1 < x_n = b$ on a given interval $[a, b]$, and the function $p(x)$ satisfies in each small interval $[x_i - 1, x_i]$ is third-order polynomial and $p(x)$ has second-order continuous derivative on the interval, the spline function is a segmented smooth function with certain smoothness at the connection of each segment. Set the cubic spline function

$$p_i(x) = A_i x^3 + B_i x^2 + C_i x + D_i. \tag{10}$$

By the definition of interpolation, then there is

$$\begin{cases} p(x_i) = y_i, p(x_i - 0) = p(x_i + 0) \\ p'(x_i - 0) = p'(x_i + 0), p''(x_i - 0) = p''(x_i + 0) \\ p'(x_0) = f'(x_0), p'(x_n) = f'(x_n). \end{cases} \tag{11}$$

According to (11), the coefficients of the corresponding interpolation function are obtained, i.e., the interpolation of the three times spline function is completed. Since the interpolation function is cubic, which basically matches with the distribution characteristics of the magnetic field.

Kriging interpolation is a commonly used method in the field of geomagnetic field estimation [29], [30], [31]. Set the estimate at a point in space (x_0, y_0) to be $\hat{z}_0$

$$\hat{z}_0 = \sum_{i=1}^{n} \lambda_i z_i. \tag{12}$$

Here, λ_{i} is the weight coefficient. It estimates the value of unknown points by using the weighted sum of the data of all known points in space. In the usual case, it is assumed that the properties of the points in the space are average, which means that the average expectation of each point on the space is set to be the same as a constant μ and the variance is set to be σ^2.

According to the unbiased estimation condition, we can further obtain

$$E(\hat{z}_0 - z_0) = E(\hat{z}_0) - E(z_0) = 0. \tag{13}$$

TABLE II
SIMULAYION PARAMETER TABLE

Parameter name	Parameter value
Outer side length	250 mm
Inner side length	110 mm
Turns	10
Wire diameter	5 mm
Excitation current	10 A

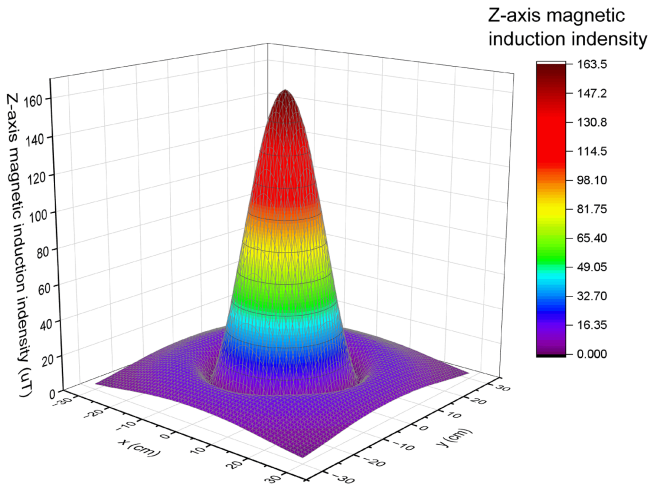

Fig. 6. Original magnetic field distribution map.

Based on the abovementioned assumptions, there are two constraints: the first constraint is

$$E\left(\sum_{i=1}^{n}\lambda_i z_i\right)-\mu=\mu\sum_{i=1}^{n}\lambda_i-\mu=0\rightarrow\sum_{i=1}^{n}\lambda_i=1. \tag{14}$$

The second constraint is to find a set λ such that make σ^2 minimizes

$$\sigma^2=S^2\left(\hat{z}_0-z_0\right)=S^2\left(\sum_{i=1}^{n}\lambda_i z_i\right)+S^2\left(z_0\right)-2\mathrm{cov}\left(\sum_{i=1}^{n}\lambda_i z_i,z_0\right). \tag{15}$$

The solution process and method of Kriging interpolation are well established and, therefore, will not be discussed here.

In this article, taking the square planar spiral coil as an example (The simulation parameters are shown in Table II.), the advantages and disadvantages of the abovementioned three interpolation methods are compared and analyzed.

The magnetic induction intensity distribution induced at a height of 15 cm from the transmitting coil, and the research area of the this coil magnetic field is – 300 mm $< x <$ 300 mm, -300 mm $< y <$ 300 mm, $z = 150$ mm. The magnetic field distribution obtained by the finite element simulation software is shown in Fig. 6.

In this article, 6 cm steps are used to simulate the actual gridded measurement steps to extract the magnetic field of this coil, and the extraction results are shown in Fig. 7. Obviously, the magnetic field extracted according to the 6 cm step has some

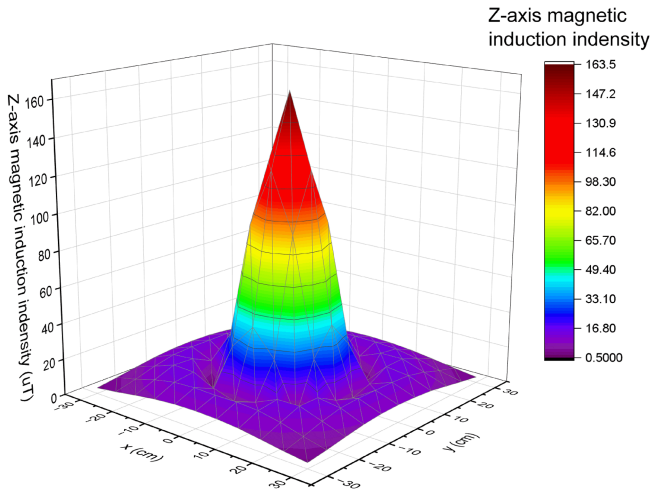

Fig. 7. Magnetic field data sampled in 6cm steps.

distortion, and need to build and restore. On the basis of Fig. 7, linear interpolation, cubic spline interpolation and Kriging interpolation methods are used to construct recovery of the simulated gridded sampled magnetic field divisions, respectively, and the grid interval of the three differentt interpolation methods is set to 1 cm.

For more visual comparison, the magnetic field data on the -300 mm $< x <$ 300 mm, $y = 0$, and $z = 150$ mm axes were taken for comparison, and the magnetic field data curves at this location, as well as the local enlargements at its top and bottom, are shown in Fig. 8.

It can be seen that linear interpolation, cubic spline interpolation and kriging interpolation can all recover the original distribution of the magnetic field to some extent well from the overall view. In the green region of Fig. 8(a)(-120 mm $< x <$ 60 mm and 60 mm $< x <$ 120 mm), the magnetic field variation is relatively linear and all three interpolation methods fit the magnetic field distribution well. In the yellow region, there is a large gap among the three fitting methods, and the most intuitive factor is the faster change in the slope of the magnetic field in this region. The local curves of the yellow region are enlarged, respectively, as shown in Fig. 8(b) and (c), and there are obvious differences in the reconstruction performance. It is obvious that in the region where the slope of the magnetic field changes rapidly, the cubic spline interpolation and Kriging interpolation can better reflect the distribution characteristics of the magnetic field, while the distortion of linear interpolation is larger.

To quantitatively evaluate the interpolation effect of various interpolation methods, the average error of interpolation, the root mean square of interpolation error, and the variance of interpolation error are introduced

$$\begin{cases}\mathrm{ME}=\sum_{i=1}^{n}\left|z_i-\hat{z}_i\right|/n\\ \mathrm{ERMS}=\sqrt{\sum_{I=1}^{n}\left(z_i-\hat{z}_i\right)^2/n}\\ \mathrm{E\,S^2}=\sum_{i=1}^{n}\left(z_i-\hat{z}_i\right)^2/n.\end{cases} \tag{16}$$

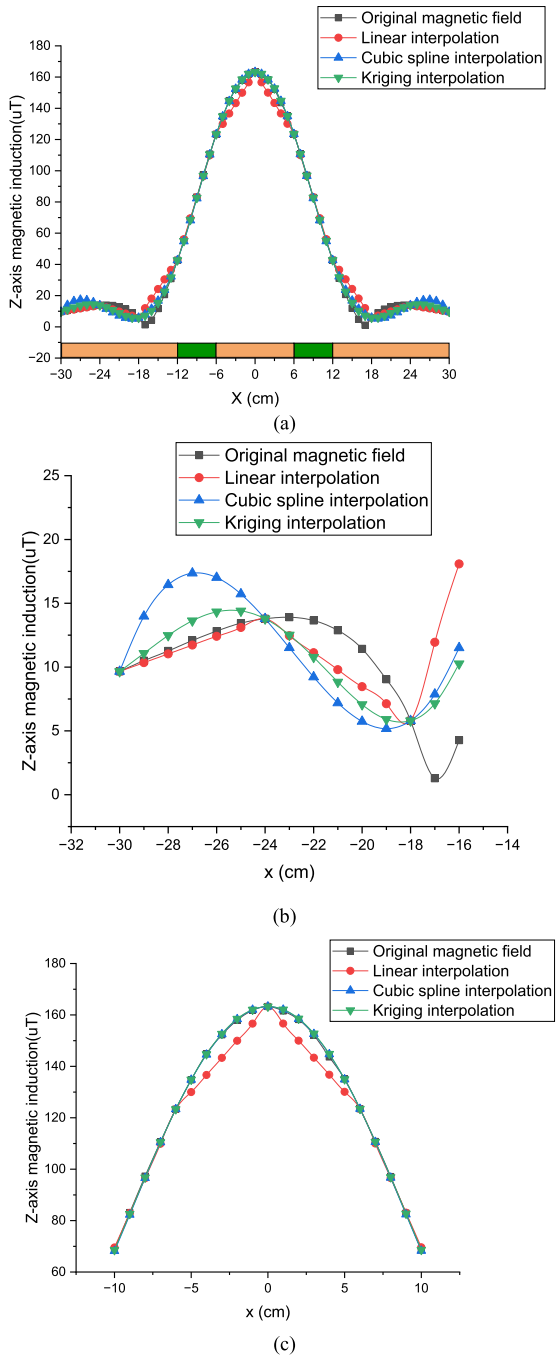

Fig. 8. (a) Coil magnetic field curve on −300 mm<x<300 mm, y = 0, z = 150 mm axis. (b) Coil magnetic field curve on −300 mm<x<160 mm, y = 0, z = 150 mm axis. (c) Coil magnetic field curve on −100 mm<x<100 mm, y = 0, z = 150 mm axis.

The error results of the three interpolation methods are shown in Table III. It can be seen that the Kriging interpolation method works best in the reconstructed reduction of the magnetic field, so kriging interpolation is used as the interpolation algorithm for magnetic field reconstruction in this article.

B. Selection and Optimization of Sampling Points

Actually, the interpolation effect of the algorithm is highly dependent on the grid division step, which means that the denser the grid sampling points are, the more accurate the interpolation result will be and the better the magnetic field recovery will be.

TABLE III
COMPARISON OF THREE INTERPOLATION METHODS

Interpolation method \ Error parameter	ME	ERMS	ES²
Linear interpolation	2.210	4.265	18.190
Cubic spline interpolation	1.578	2.533	6.415
Kriging interpolation	1.388	2.173	4.723

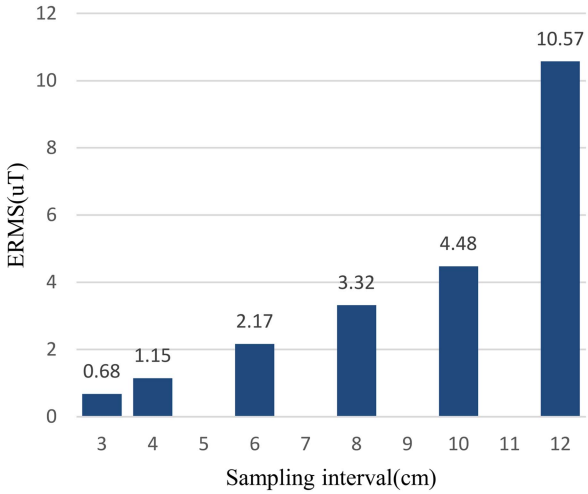

Fig. 9. Effect of different magnetic field sampling intervals on reconstruction accuracy.

Taking the magnetic field distribution of the model shown in Table II as an example, the magnetic fields were resampled at intervals of 3 cm, 4 cm, 6 cm, 8 cm, 10 cm, and 12 cm, respectively. Kriging interpolation was used to reconstruct the magnetic field, and the interpolation error was calculated according to (16). In Fig. 9, the root-mean-square error of the reconstruction results is the best when the sampling interval is small. Therefore, if conditions permit, the sampling interval should be reduced as much as possible.

Compared to the original magnetic field, the results of the reconstructed magnetic field though the Kriging interpolation also have a large error with the sampling interval is 12 cm, as shown in Fig. 10.

Therefore, in practice, it is defective to use an equal fraction of magnetic field for gridded data acquisition. The overall magnetic field interpolation can be effectively improved by increasing the sampling density in the region with large magnetic field variability. In this article, the second-order rate of change of the sampled magnetic field is used as the evaluation index. It is defined that when the second-order rate of change of the fitted magnetic field is between −0.005 and 0.005, it is the region of small magnetic field rate of change, and the other regions are the regions of large magnetic field rate of change. Of course, the threshold setting of the second order rate of change can also be determined according to the actual positioning accuracy requirements.

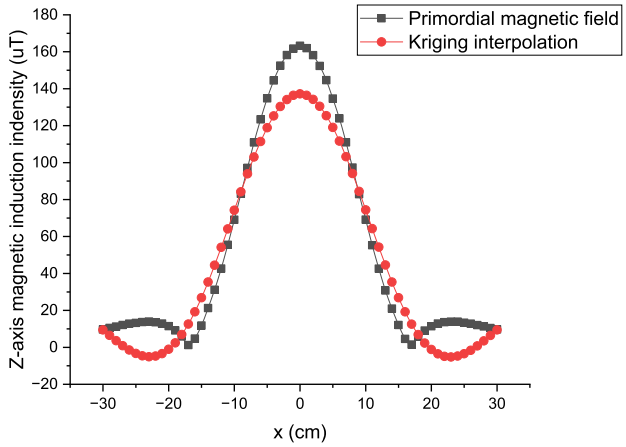

Fig. 10. Results of the reconstructed magnetic field compared with the simulated magnetic field with a sampling interval of 12 cm.

Since the induced voltage of the pickup coil is in one-to-one correspondence with the z-axis magnetic flux density, the method of converting the magnetic field reconstruction into the reconstruction of the induced voltage can be more effectively applied to coil positioning.

IV. Simulation and Experimental Verification

A. Simulation Verification

The coil size model used in the simulation refers to the WPT2-Z2 structure in the SAE J2954 standard, with an excitation current of 10 A, and frequency of 85 kHz. The gyroscope is mounted at the center of the secondary coil, the pickup coil is mounted at the center of the four sides of the receiving coil, and the distance d between the pickup coils mounted on opposite sides is 16 cm. The simulation flow chart is shown in Fig. 11.

1) The finite element method is used to calculate the above-mentioned model. Taking z as 15 cm, Bz of magnetic flux density in the range of 60 cm × 60 cm in XY plane is calculated. Since the magnetic flux density is reflected by the pickup coil induced voltage, the magnetic induction strength data is multiplied by a fixed factor to obtain the pickup coil induced voltage U_{di} under the corresponding magnetic field, which is used to simulate as the actual pickup coil voltage.
2) Simulates the measurement process of the pickup coil voltage at the actual grid. The voltage in the plane of the transmitting coil is sampled in a grid with a valid interval of 3 cm, and a total of 441 data points are sampled. The sampled voltage values are subsequently reconstructed and expanded using the Kriging interpolation. The reconstructed data step is set to 1 cm, the reconstructed data points are increased to 3721, and the minimum spacing between grid points is 1 cm.
3) Calculates the position coordinates in MATLAB. Considering the actual possible error, a certain random error is set for the angle data to improve the authenticity and applicability of the simulation. And the parking deviation of electric vehicles generally does not exceed 30° in practice, the value of θ^0 is set at $-30°\sim30°$. Though the positioning algorithm model described in this article, the simulation results are shown in Table IV.

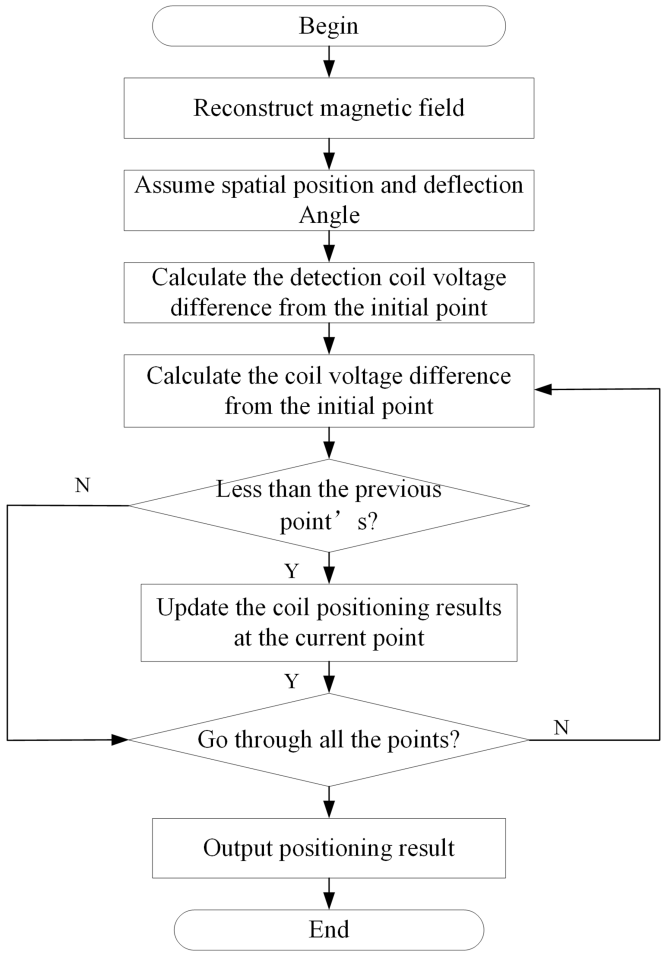

Fig. 11. MATLAB simulation program flow chart.

TABLE IV
Simulation Result Data

NO.	Theoretical value (x(cm),y(cm))/ $\theta°$	Before Reconstruction	After Reconstruction
		Simulation value (x,y)/ $\theta°$	Simulation value (x,y)/ $\theta°$
1	(-3.1, -10.6)/ 5.3	(-3.8, -9.2)/ 5.7	(-2.3, -11.1)/ 5.7
2	(-17.2, -8.5)/ 5.6	(-15.6, -9.6)/ 6.1	(-17.4, -9.2)/ 6.1
3	(-10.0, 3.0)/ -7.0	(-9.1,2.3)/ -6.9	(-10.5, 3.2)/ -6.9
4	(-10.4, 15.9)/ 0.0	(-8.9, 14.7)/ 0.4	(-10.9, 16.1)/ 0.4
5	(7.3, 9.6)/ 2.0	(5.6, 7.3)/ 2.1	(8.1, 9.4)/ 2.1
6	(18.5, 6.0)/ -6.6	(18.0, 4.2)/ -8	(18.4, 7.0)/ -8
7	(3.5, -9.0)/ -18.0	(2.4, -7.9)/ -16.6	(2.8, -9.3)/ -16.6
8	(14.7, -7.7)/ 24.0	(12.1, -6.4)/ 25.5	(14.3, -8.1)/ 25.5
9	(0.5,1.5)/ 9.0	(0.1, 3.1)/ 8.1	(0.1, 2.4)/ 8.1
10	(2.4, 0.0)/ -15.0)	(3.2, 0.8)/ -15.6	(2.1, 0.1)/ -15.6

In order to evaluate the effectiveness of localization, we introduce positioning error to evaluate the positioning results. Suppose (x_a, y_a) is the actual coordinate and (x_p, y_p) is the

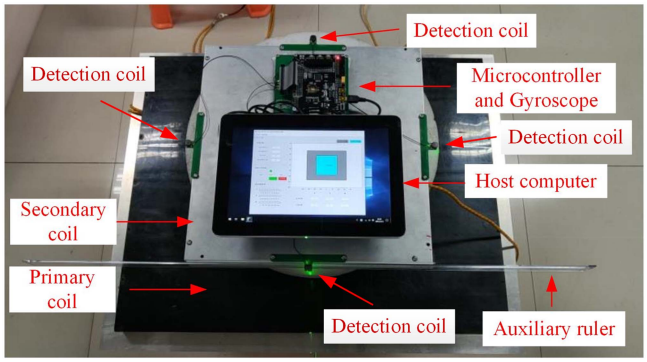

Fig. 12. Wireless charging coil positioning system experimental device and detection coil.

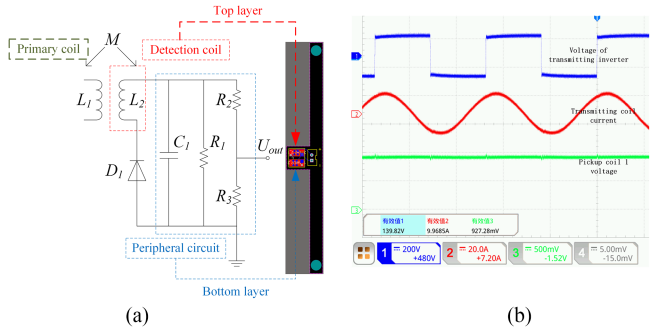

Fig. 13. Pickup coil circuit and experiment parameters waveform. (a) Pickup coil circuit. (b) Experiment waveform.

TABLE V
SIMULATION PARAMETER TABLE

Parameter name	Parameter value
Transmitting/ Receiving coil	WPT2-Z2/ SAE J2954
Pickup coil radius	8.5 mm
Pickup coil inductance L_2	100 μH
R_1, R_2, R_3	10 kΩ,1 kΩ,2 kΩ
$C1$	10 μF
Distance between transmitting and receiving coils Plane Z	20 cm
Positioning processor	STM32F103RCT6
Rotation angle attitude sensor (gyroscope)	HWT101

TABLE VI
RESULTS OF EXPERIMENTS WITH SAMPLING INTERVAL OF 5 CM

NO.	Actual x(cm),y(cm),θ(°)	Positioning x (cm),y(cm),θ(°)	Error e_{max}(cm),Δθ(°)
1	-3.1, -10.6, 5.3	-5.0, -10.0, 5.0	1.99 0.3
2	-17.2, -8.5, 5.6	-18.0, -9.0, 6.0	0.94 0.4
3	-10.0, 3.0, -7.0	-11.0, 3.0, -7.5	1.00 0.5
4	-10.4, 12.2, 0.0	-14, 10, 0.9	4.21 0.9
5	7.3, 9.6, 2.0	8.0, 8.0, 1.8	1.75 0.2
6	18.5, 6.0, -6.6	19.0, 7.0, -8.0	1.12 1.4
7	3.5, -9.0, -18.0	-2.0, -9.0, -17.1	5.50 0.9
8	14.7, -7.7, 24.0	16.0, -6.0, 21.0	2.14 3.0
9	0.5, 1.5, 9.0	4.0, 2.0, 8.9	3.54 0.1
10	2.4, 0.0, -15.0	4.0, 1.0, -14.3	1.89 0.7

positioning coordinate. Define

$$\Delta x = |x_a - x_p| \ \Delta y = |y_a - y_p| \ e = \sqrt{\Delta x^2 + \Delta y^2}. \quad (17)$$

It is not difficult to see that the maximum error of positioning with raw data is 2.9 cm, and the average error is 1.8 cm when the angle deflection between the receiving and transmitting coils is within 30° and the sampling interval is 3 cm. After reconstruction and expansion of the sampled voltage value, the maximum positioning error is reduced to 1 cm, and the average error is reduced to 0.72 cm, which effectively verifies the effectiveness of the method in this article.

B. Experimental Verification

WPT platform with *LCC*-S topology compensation is built for verification (as shown in Fig. 12). However, since no power is transmitted during the positioning process, this positioning method can also be applied to other topology compensation. Parameters of system are shown in Table V. In fact, *LCC* topology is adopted at the transmitting coil to ensure constant current characteristics, which is widely used. The pickup coils and it is processing circuit are shown in Fig. 13(a). During positioning, the receiving coil is disconnected. The current of the transmitting coil is stabilized at 10 A and the frequency at 85 kHz square wave by adjusting the system input [as shown in Fig. 13(b)].

At the beginning of the experiment, in order to verify the influence of the deflection angle of the receiving coil on the point where the same pickup coil is located within the allowable deviation range, we take the actual receiving coil with four pick-up coils to sample and measure. The position of one pickup-coil is fixed and the receiving coil is rotated for voltage acquisition. The experimental waveform is shown in Fig. 14. It can be seen that the induced voltage at the fixed sampling grid will change when the deflection angle changes, however, within the allowable deviation range of electric vehicles, the impact is not obvious. Ignore or average value at different angles can be used for sampling. In the experiment, the grid point induction voltage data sampling is performed at the beginning. The sampling interval is set to 5 cm, and the sampling range of the grid point of the transmitting coil is -30 cm $\leq x \leq 30$ cm, -20 cm $\leq y \leq 20$ cm. Due to the symmetry of the transmitting coil, the magnetic field area of the transmitting coil is divided into four quadrants, the number of voltage sampling points is 35, as shown in Fig. 15(a), and the values of the remaining quadrants are complemented by mirror symmetry. The sampled pickup coil voltage values are reconstructed by Kriging interpolation as described in the article with 1 cm reconstruction step to obtain the constructed voltage distribution, as shown in Fig. 15(b).

With an angular offset of 0–30° in the y-axis of the offset test plane as a constraint, ten positions, and directions are randomly selected for the positioning experiments. The positioning experimental results are shown in Table VI. It shows that when the sampling interval is set to 5 cm, the maximum positioning error of 10 randomly selected experiments is 5.5 cm is large than expected error. In this experiment the average positioning error is 2.4 cm. Main reasons for error is that the receiving coil has a certain influence on the voltage of the pickup coil, and the gyroscope also has errors in angle measurement.

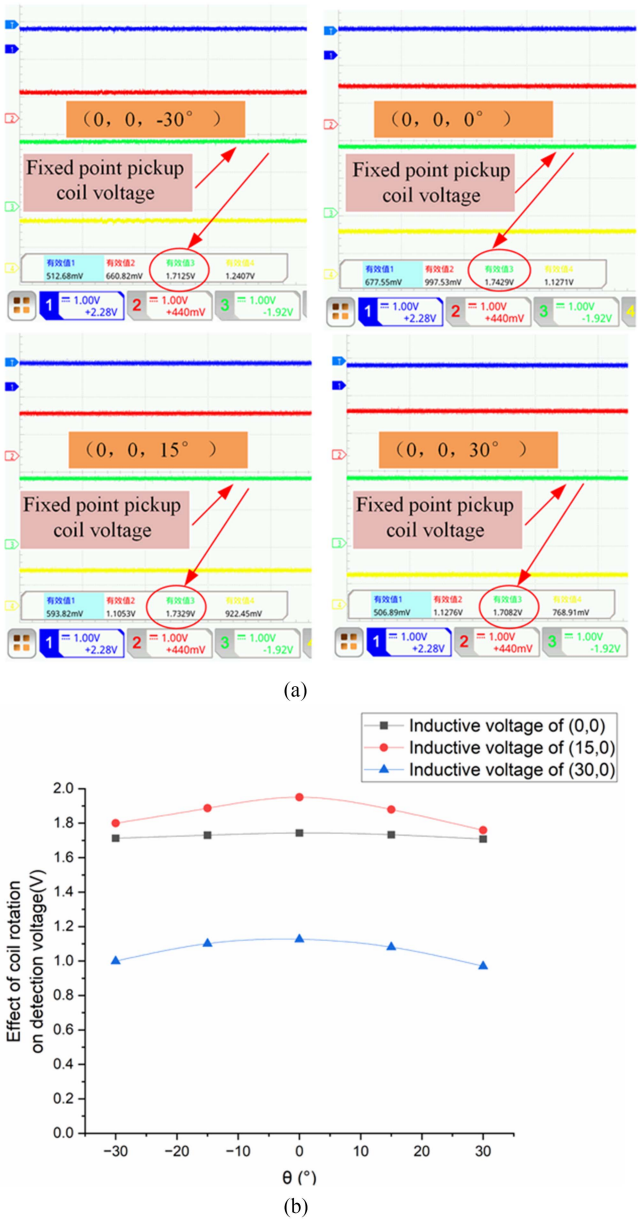

Fig. 14. Pick-up coil voltage with different receiving coils' angle. (a) Waveform of deflection effect on Pick-up coil voltage at a fixed point. (b) Pick-up coil voltage with different deflection angle at different position.

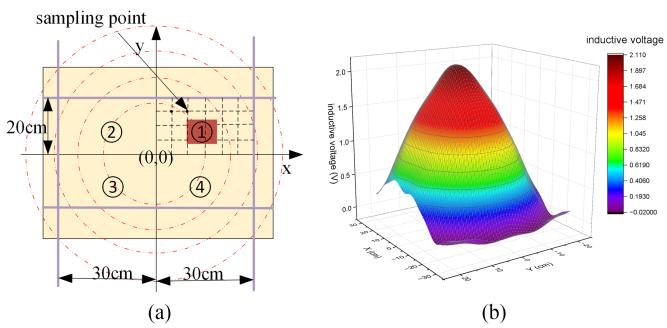

Fig. 15. Grid sampling partition and voltage results reconstructed in the experiment. (a) Grid sampling partition. (b) Voltage results reconstructed.

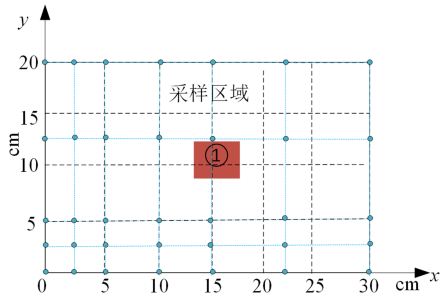

Fig. 16. Sampling points in the sampling interval before and after optimization (grid point coordinates are reset to x = 0 cm, x = 2.5 cm, x = 5 cm, x = 10 cm, x = 15 cm, x = 22.5 cm, x = 30 cm, y = 0 cm, y = 2.5 cm, y = 5 cm, y = 12.5 cm, y = 20 cm).

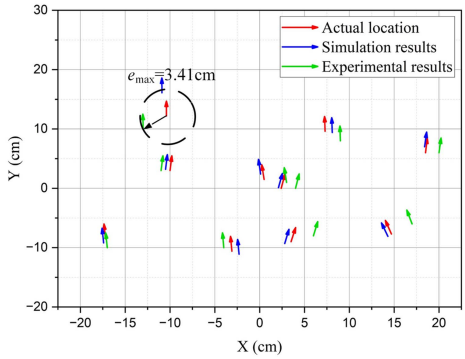

Fig. 17. Experimental results of the optimized sampling method.

Here, the maximum error in angle measurement is about 3° and the average error is less than 1° from Fig. 14(b), but these errors are hard to be avoided.

In the second experiment, the reconstruction accuracy of induced voltage is improved by optimizing the sampling interval. There are still 35 grid sampling points in the first quadrant, but the distance between the sampling points is adjusted according to the distribution characteristics of the magnetic field change rate and the grid point spacing is adjusted, as shown in Fig. 16. The principle of adjustment is to set more sampling points in the region with high magnetic field variation rate and less sampling points in other regions.

Then, the collected voltage of grid point is also reconstructed according to the 1 cm grid spacing, and the results of the repositioning experiment are shown in Fig. 17. The starting point of the arrow indicates the X,Y position, and the direction of the arrow depicts the deflection angle of the transmitting and the receiving coil in Fig. 17. Compared with Table VI, the maximum positioning error is less than 3.4 cm with the same number of sampling points, and the average positioning error is small to 2.1 cm. It shows that the method of variable slope interval sampling is feasible. Finally, in the equally spaced grid sampling, we shortened the grid interval from the original 5 cm to 2.5 cm, i.e., 117 sampling points are sampled in the first quadrant. The step size after reconstruction is still 1 cm. At the same location, 10 positioning comparison experiments are conducted again, and the positioning experiment result is shown

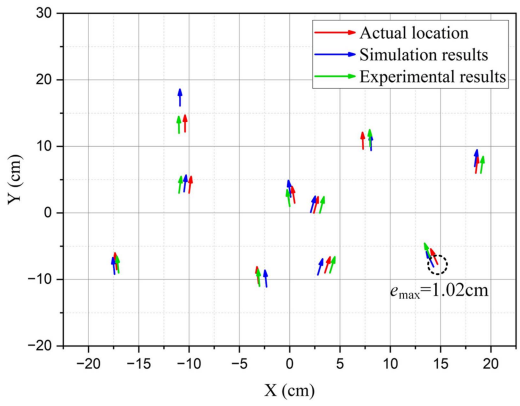

Fig. 18. Results of optimization experiments with 2.5 cm sampling interval.

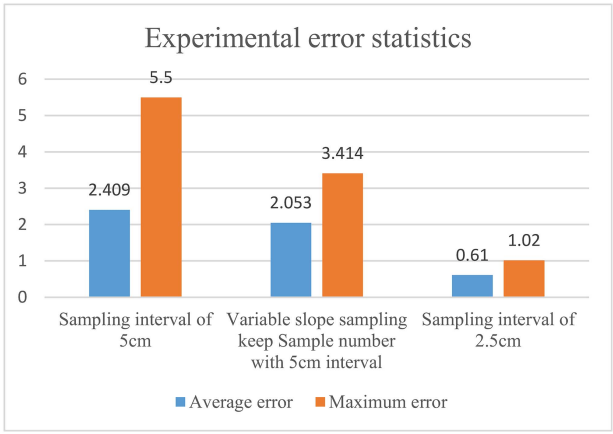

Fig. 19. Error comparison of the three experiments.

in Fig. 18. It is not difficult to find that the maximum positioning error is increased from 5.5 cm to 1.02 cm, and the average positioning error is reduced to 0.61 cm. The error comparison of the three experiments is shown in Fig. 19.

The experimental results show that the abovementioned two measures are helpful to reduce the positioning error. It is not difficult to find that reducing the grid point sampling interval is more effective in improving the positioning accuracy, and the sampling optimization method with variable slope can also further improve the positioning accuracy while keeping the number of sampling points unchanged. Sometimes, those two methods can be combined in practice.

V. Conclusion

In this article, the reason of the positioning failure of the existing localization algorithm is analyzed when the coil angle rotates under the symmetrical magnetic field, and the positioning constraint equation for coils with angle is established. On this basis, a gridded positioning strategy of the coupling mechanism of the WPT system with offset angle variable is proposed. The secondary coordinates of the positioning results is no longer corrected in this article, but the Kriging interpolation method is used to reconstruct pick-up coil voltages, and the positioning accuracy is effectively improved by reconstructing the grid sampling point voltage distribution. Two methods are designed and verified, respectively, to improve the positioning accuracy.

In the implementation process of this article, according to the experimental analysis, the influence of the rotation of the receiving coil on the pickup-coil voltage at the sampling point is ignored, which has certain limitations and is the main reason for the positioning error. Also, the research did not consider the possible variations in the *Z*-axis direction of the receiving and transmitting coils, although the distance between the transmitting coil and the receiving coil of the electric vehicle varies little in practice, there is still the possibility of change. Therefore, further research around the abovementioned areas will continue to follow in order to improve the generality of this positioning method.

References

[1] Z. Wei and B. Zhang, "Transmission range extension of PT-Symmetry-Based wireless power transfer system," *IEEE Trans. Power Electron.*, vol. 36, no. 10, pp. 11135–11147, Oct. 2021.

[2] SAE standard J2954TM, "Wireless power transfer for light-duty plug-in/electric vehicles and alignment methodology," Oct. 2020. [Online]. Available: https://www.sae.org/standards/content/J2954 202010

[3] S. A. Birrell, D. Wilson, C. P. Yang, G. Dhadyalla, and P. Jennings, "How driver behavior and parking alignment affects inductive charging systems for electric vehicles," *Transp. Res. C Emerg. Technol.*, vol. 58, pp. 721–731, Sep. 2015.

[4] X. Huang, J. Xu, C. Xu, Y. Wu, and X. Li, "Design of magnetic coupling mechanism with gentle excursion performance for wireless power transfer system," in *Proc. IEEE 6th Asia Conf. Power Elect. Eng.*, 2021, pp. 1466–1470.

[5] H. Zhang, Y. Chen, C. -H. Jo, S. -J. Park, and D. -H. Kim, "DC-Link and switched capacitor control for varying coupling conditions in inductive power transfer system for unmanned aerial vehicles," *IEEE Trans. Power Electron.*, vol. 36, no. 5, pp. 5108–5120, May 2021.

[6] G. A. Covic and J. T. Boys, "Modern trends in inductive power transfer for transportation applications," *IEEE J. Emerg. Sel. Topics. Power Electron.*, vol. 1, no. 1, pp. 28–41, Mar. 2013.

[7] S. M. Lee, "Ultrawideband (UWB)-based precise short-range localization for wireless power transfer to electric vehicles in parking environments," *Peer J Comput. Sci.*, vol. 7, no. 9, 2021, Art. no. e567.

[8] J. Tiemann, J. Pillmann, S. Bocker, and C. Wietfeld, "Ultra-Wideband aided precision parking for wireless power transfer to electric vehicles in real life scenarios," in *Proc. IEEE 84th Veh. Technol. Conf.*, 2016, pp. 1–5.

[9] S. Malhotra and M. Hashmi, "Near-field WPT using defected ground structures for UHF RFID applications," in *Proc. IEEE Int. Conf. RFID Technol. Appl.*, 2019, pp. 16–21.

[10] Y. Zhang, L. Hsiung-Cheng, J. Zhao, M. Zewen, Z. Yem, and H. Sun, "A multi-DoF ultrasonic receiving device for indoor positioning of AGV system," in *Proc. IEEE Int. Symp. Comput., Consum. Control*, 2018, pp. 97–100.

[11] J. Aparicio, A. Jiménez, F. J. Álvarez, D. Ruiz, C. De Marziani, and J. Ureña, "Characterization of an underwater positioning system based on GPS surface nodes and encoded acoustic signals," *IEEE Trans. Instrum. Meas.*, vol. 65, no. 8, pp. 1773–1784, Aug. 2016.

[12] Y. Zhang, L. Hsiung-Cheng, J. Zhao, M. Zewen, Z. Ye, and H. Sun, "A Multi-DoF ultrasonic receiving device for indoor positioning of AGV system," in *Proc. Int. Symp. Comput., Consum. Control*, 2018, pp. 97–100.

[13] R. Yan, Z. Qian, J. Wu, and X. He, "Magnetic coupling positioning using simultaneous power and data transfer," in *Proc. IEEE IECON 44th Annu. Conf. Ind. Electron. Soc.*, 2018, pp. 4822–4827.

[14] W. Han, K. Chau, C. Jiang, and W. Liu, "Accurate position detection in wireless power transfer using magnetoresistive sensors for implant applications," in *Proc. IEEE Int. Magn. Conf.*, 2018, pp. 1–1.

[15] Y. Gao et al., "Magnetic alignment detection using existing charging facility in wireless EV chargers," *J. Sensors*, vol. 2016, 2016, Art. no. 5670510.

[16] I. Cortes and W. -J. Kim, "Lateral position error reduction using misalignment-sensing coils in inductive power transfer systems," *IEEE-ASME T Mech*, vol. 23, no. 2, pp. 875–882, Apr. 2018.

[17] I. Cortes and W. -J. Kim, "Automated alignment with respect to a moving inductive wireless charger," *IEEE Trans. Transp. Electr.*, vol. 8, no. 1, pp. 605–614, Mar. 2022.

[18] L. Tan et al., "Mesh-Based accurate positioning strategy of EV wireless charging coil with detection coils," *IEEE Trans. Ind. Inform*, vol. 17, no. 5, pp. 3176–3185, May 2021.
[19] W. Wang, C. Zhang, J. Wang, and X. Tang, "Multipurpose flexible positioning device based on electromagnetic balance for EVs wireless charging," *IEEE Trans. Ind. Electron.*, vol. 68, no. 10, pp. 10229–10239, Oct. 2021.
[20] B. Zhang et al., "Triple-Coil-Structure-Based coil positioning system for wireless EV charger," *IEEE Trans. Power Electron.*, vol. 36, no. 12, pp. 13515–13525, Dec. 2021.
[21] M. X. Zou, Z. Cong, and J. Xu, "A new coil structure for positioning estimate of wireless power transmission," *Int. J. RF Microw. Comput. Aided Eng.*, vol. 30, no. 12, pp. 1–14, 2020.
[22] F. Wen, X. Chu, Q. Li, W. Zhao, X. Zhu, and Y. Wu, "Receiver localization strategy of wireless charging system based on mutual inductance disturbance," *IEEE Trans. Appl. Supercond.*, vol. 31, no. 8, Nov. 2021, Art. no. 0600604.
[23] Z. Liu et al., "Receiver position identification method of wireless power transfer system based on magnetic integration inductance," *IEEE Trans. Ind. Appl.*, vol. 58, no. 1, pp. 1136–1145, Jan./Feb. 2022.
[24] W. Hijikata and H. Suzuki, "Real-time optimization of coil positioning in wireless power transfer system for artificial heart," in *Proc. IEEE Wireless Power Transfer Conf.*, 2018, pp. 1–4.
[25] V. H. Nguyen and W. -j. Kim, "Two-Phase Lorentz coils and linear halbach array for multiaxis precision-positioning stages with magnetic levitation," *IEEE/ASME Trans. Mechatronics*, vol. 22, no. 6, pp. 2662–2672, Dec. 2017.
[26] Y. Shin, K. Hwang, J. Park, D. Kim, and S. Ahn, "Precise vehicle location detection method using a wireless power transfer (WPT) system," *IEEE Trans. Veh. Technol.*, vol. 68, no. 2, pp. 1167–1177, Feb. 2019.
[27] S. Y. Jeong, H. G. Kwak, G. C. Jang, S. Y. Choi, and C. T. Rim, "Dual-purpose nonoverlapping coil sets as metal object and vehicle position detections for wireless stationary EV chargers," *IEEE Trans. Power Electron.*, vol. 33, no. 9, pp. 7387–7397, Sep. 2018.
[28] J.-H. Ahn and B. K. Lee, "High-efficiency adaptive-current charging strategy for electric vehicles considering variation of internal resistance of lithium-ion battery," *IEEE Trans. Power Electron.*, vol. 34, no. 4, pp. 3041–3052, Apr. 2019.
[29] Y. H. Chen, Y.Z. Xie, M. Z. Liu, Z. Y. Wang, Q. Liu, and A. C. Qiu, "Geomagnetically induced current calculation of high voltage power system with long transmission lines using kriging method," *IEEE Trans. Power Del.*, vol. 37, no. 1, pp. 650–657, Feb. 2022.
[30] H. Wang, T. Jiang, Y. Li, Y. Li, F. Ye, and B. Cao, "Research on electromagnetic positioning calibration technology based on Kriging interpolation," in *Proc. IEEE Int. Symp. Antennas Propag. USNC-URSI Radio Sci. Meeting*, 2019, pp. 769–770.
[31] L. Bolduc, P. Langlois, D. Boteler, and R. Pirjola, "A study of geoelectromagnetic disturbances in Québec. 1. General results," *IEEE Trans. Power Del.*, vol. 13, no. 4, pp. 1251–1256, Oct. 1998.

Linlin Tan (Member, IEEE) received the B.S. degree in electrical engineering and automation from Harbin Engineering University, Harbin, China, in 2008, and the Ph.D. degree in electrical engineering from Southeast University, Nanjing, China, in 2014.

He is currently an Associate Professor with the School of Electrical Engineering, Southeast University, Nanjing, China. He has authored or coauthored more than 30 papers and more than 40 inventions. His research interests include wireless power transfer, wireless charging for electric vehicles, and wireless V2G

Yongfeng Yu was born in Anhui, China, in 1999. He received the B.S. degree in 2021 from Southeast University, Nanjing, China, where he is currently working toward the M.S. degree both in electrical engineering.

His research interests include wireless power transfer, coil positioning technology, and control of BD-WPT system.

Jiaqi Wang received the B.S. degree in electrical engineering and automation from the College of Electrical and Automation Engineering, Nanjing Normal University, in 2022. She is currently working toward the M.S. degree in electrical engineering from Southeast University, Nanjing, China.

Her current research interests include parameter measurement, topology, and control of electric vehicle wireless charging.

Ruoyin Wang was born in Zhenjiang, China, in 1991. He received the M.S. degree from Jiangsu University, Zhenjiang, China, in 2018. He is currently working toward the Ph.D. degree with Southeast University, Nanjing, China, both in electrical engineering.

His research interests include wireless power transfer, wide bandgap power devices, coil positioning, and temperature control technology.

Chengyun Li was born in Shandong, China, in 1997. He received the B.S. and M.S. degrees in electrical engineering from Southeast University, Nanjing, China, in 2019 and 2022, respectively.

His research interests include wireless power transfer, coil positioning technology, and high-efficiency power technology.